Inorg. Chem. **2004**, *43*, 1116–1121

Density Functional Theory Study of the d^{10} Series $(H_3P)_3M(\eta^1\text{-}SO_2)$ and $(Me_nPh_{3-n}P)_3M(\eta^1\text{-}SO_2)$ (M = Ni, Pd, Pt; n = 0–3): SO_2 Pyramidality and M–S Bond Dissociation Energies

Daniel J. Brust and Thomas M. Gilbert*,[1]

Department of Chemistry and Biochemistry, Northern Illinois University, DeKalb, Illinois 60115

Received July 16, 2003

Quantum mechanical density functional theory (DFT) and coupled DFT/molecular mechanics (QMMM) studies of the compounds $(H_3P)_3M(\eta^1\text{-}SO_2)$ and $(Me_nPh_{3-n}P)_3M(\eta^1\text{-}SO_2)$ (M = Ni, Pd, Pt; n = 0–3) model the experimental data well, particularly the planar/pyramidal geometries at sulfur. Bond dissociation energy (BDE) calculations confirm that Pd/Pt systems with pyramidal SO_2 ligands exhibit M–S BDEs smaller by 30–50% than Ni systems with planar SO_2. However, scans of the potential energy surfaces show that flexing the planar/pyramidal torsion angle within ranges of 20–30° requires little energy. Bond energy decomposition calculations indicate that the electrostatic ΔE_{elstat} term determines the BDE for Pd/Pt molecules where the sulfur is pyramidal, whereas all three terms matter when the sulfur is planar, as for Ni compounds. However, this accounts only for a fraction of the BDE differences; orbital energy matching accounts for the balance.

Introduction

The d^{10} tris(phosphine)M(η^1-SO_2) complexes (M = Ni, Pd, Pt) exhibit intriguing chemical and physical behavior. For example, $(Ph_3P)_3Pt(\eta^1$-pyramidal $SO_2)$ reacts with molecular oxygen to form $(Ph_3P)_2Pt(SO_4)\cdot H_2O$,[2] while $(Ph_3P)_3$-Ni(η^1-nearly planar SO_2) does not.[3] Kubas et al. suggested a correlation between the pyramidality of the SO_2 ligand and its lability in these species.[4] Spectroscopic and crystallographic data indicate that $(Ph_3P)_3Ni(\eta^1\text{-}SO_2)$ and $(Cy_3P)_3$-$Ni(\eta^1\text{-}SO_2)$ contain planar (or nearly so) SO_2 ligands, while $(Me_2PhP)_3Ni(\eta^1\text{-}SO_2)$ contains a pyramidal SO_2 ligand.[5,6] Semiquantitative theoretical studies bear out this bonding flexibility.[4,7] More quantitative ab initio computational modeling studies of the area are limited to the work of Sakaki et al. on $(H_3P)_3Ni(\eta^1\text{-}SO_2)$.[8]

Despite these and other efforts, determining whether the SO_2 ligand binds in a planar or pyramidal fashion remains difficult. Furthermore, the quantitative energetics of the preference remain unexplored. It would prove useful to know how much stronger a bond between a metal and a planar SO_2 ligand is than one between a metal and a pyramidal SO_2. Similarly, quantitative understanding of the relationship between the metal−sulfur bond strength and the reactivity of the SO_2 ligand would be welcome.

We have begun a program involving computational modeling of transition metal catalysts that can convert SO_2 into less poisonous and/or more commercially useful materials such as sulfur or sulfates. As part of this, we previously investigated the bond dissociation energies (BDEs) of a variety of L_5M-SO_2 complexes (L = CO, NH_3) in the hope of correlating bond energy with reactivity.[9] We report here quantum mechanical density functional theory (DFT) and coupled DFT/molecular mechanics (QMMM) studies of the d^{10} compounds $(H_3P)_3M(\eta^1\text{-}SO_2)$ and $(Me_nPh_{3-n}P)_3M(\eta^1$-$SO_2)$ (M = Ni, Pd, Pt; n = 0−3). Our goals for the studies were (1) to examine the energetics of pyramidality/planarity of SO_2 in such complexes to see how difficult it is to interconvert the two conformational types; (2) to determine how much stronger a metal−(η^1-planar SO_2) bond is than a

* Author to whom correspondence should be addressed.
(1) E-mail: tgilbert@marilyn.chem.niu.edu.

(2) Levison, J. J.; Robinson, S. D. *J. Chem. Soc., Dalton Trans.* **1972**, 2013−2017.
(3) Moody, D. C.; Ryan, R. R. *Inorg. Chem*. **1979**, *18*, 223−227.
(4) Ryan, R. R.; Kubas, G. J.; Moody, D. C.; Eller, P G. *Struct. Bonding* **1981**, *46*, 47−100.
(5) (a) Schimmelpfennig, U.; Kalähne, R.; Schleintz, K. D.; Wenschuh, E. *Z. Anorg. Allg. Chem.* **1991**, *603*, 21−24. (b) Hoffmann, T.; Hoffmann, H.; Karabit, M.; Zdunneck, P.; Wenschuh, E.; Reinhold: J.; Schüler, M. *Z. Anorg. Allg. Chem*. **1988**, *565*, 91−105.
(6) Sieler, J.; Peters, K.; Wenschuh, E.; Hoffmann, T. *Z. Anorg. Allg. Chem*. **1987**, *549*, 171−176.
(7) Reinhold, J.; Schüler, M.; Sieler, J.; Hoffmann, T.; Wenschuh, E. *Z. Chem*. **1988**, *28*, 74−75.
(8) Sakaki, S.; Sato, H.; Imai, Y.; Morokuma, K.; Ohkubo, K. *Inorg. Chem*. **1985**, *24*, 4538−4544.
(9) (a) Retzer, H. J.; Gilbert, T. M. *Inorg. Chem*. **2003**, *42*, 7207−7218. (b) Gilbert, T. M., to be published.

10.1021/ic030229q CCC: $27.50
Published on Web 01/15/2004

(η^1-pyramidal SO_2) bond; (3) to determine whether phosphine basicity and the BDEs are related; and (4) to examine the BDEs for trends/values that might be related to their reactivities. The data suggest considerable similarity between complexes of a particular metal, with curious trends as the phosphine ligands change. The SO_2 ligand exhibits considerable flexibility in its bonding because the energies separating planar and pyramidal conformations and staggered and eclipsed orientations are small.

Computational Details

General. All DFT calculations were carried out using the Amsterdam Density Functional (ADF) program[10] developed by Baerends et al.[11] and vectorized by Ravenek.[12] The numerical integration scheme applied for the calculations was developed by te Velde et al.;[13] the geometry optimization procedure derives from that of Versluis and Ziegler.[14] Geometry optimizations were carried out using the local density approximation of Vosko, Wilk, and Nusair (LDA VWN)[15] augmented with the nonlocal gradient correction PW91 from Perdew and Wang.[16] Relativistic corrections were added using a scalar-relativistic zeroth order relativistic approximation (ZORA) Hamiltonian.[17,18] The electronic configurations of the molecular systems were described either by a triple-ζ + polarization (TZP) basis set for all atoms [$(H_3P)_3M$ and $(Me_3P)_3M$ series] or by a mixed basis set where the TZP basis set was used on the metal, S, O, and P, while a double-ζ basis set (DZ) was used on C and H [$(Me_2PhP)_3M$, $(Ph_2MeP)_3M$, and $(Ph_3P)_3M$ series]. The motivation for the latter choice is described below. Non-hydrogen atoms were assigned a relativistic frozen core potential, treating as core the shells up to and including the following: 1s for O and C, 2p for first-row transition metals, P, and S, 3d for second-row metals, 4d for third-row metals. A set of auxiliary s, p, d, and f functions, centered on all nuclei, was used to fit the molecular density and represent Coulomb and exchange potentials accurately in each SCF cycle.

QMMM Studies. Coupled DFT/molecular mechanics (QMMM) optimizations were performed using the QMMM module within ADF. The included SYBYL force field[19] was employed for the MM portion of the calculations. Parameters for Ni, Pd, and Pt atoms were added from the UFF force field.[20] Running QMMM calculations with ADF requires input of the parameter α, which represents the ratio of the bond length between QM and MM link atoms in the "true" compound to the bond length between QM and "model" atoms. For the molecules studied here, where the alkyl/aryl phosphines were modeled as PH_3, this means the ratio between the P−C (phenyl or methyl) bond length and the P−H bond length. An appropriate value for α was determined by optimizing $(Ph_3P)_3Ni(\eta^1\text{-}SO_2)$ using QMMM with the TZP basis set and various values of α, and examining the optimized P−C (phenyl) bond length. The data appear in Table 1. A value of $\alpha = 1.27$ gives excellent agreement with the experimental average P−C distance of 1.843 Å. Use of this value is substantiated by the agreement between experimental and calculated P−C distances in other $(R_3P)_3M$ and $(R_3P)_3M(\eta^1\text{-}SO_2)$ molecules for which experimental data exist.[21] The value of α has little effect on the parameters within the QM portion of the molecule, which are of the greatest interest here.

Table 1. Selected Predicted (PW91, QMMM) Structural Data for $(Ph_3P)_3Ni(\eta^1\text{-}SO_2)$ Using Various Values of α[a]

α	P−C (av)	Ni − S	$\tau_{Ni\ SO_2}$[b]
1.20	1.746	2.100	161.1
1.25	1.811	2.097	160.9
1.27	1.840	2.091	161.3
1.28	1.850	2.094	161.1
1.30	1.879	2.087	163.8
expt	1.843	2.038(4)	166.9

[a] Distances are in Å, angles in deg. [b] $\tau_{Ni\ SO_2}$ is the angle between the Ni−S bond vector and the plane containing the SO_2 atoms.

The QMMM approach was employed for two areas of study: the SO_2 conformation/orientation scans of $(Ph_2MeP)_3M(\eta^1\text{-}SO_2)$ and $(Ph_3P)_3M(\eta^1\text{-}SO_2)$ (see below), where pure DFT studies would have been resource-prohibitive, and to examine several (typically 8−10) possible conformations of the phenyl and methyl groups in the $(Me_nPh_{3-n}P)_3M$ and $(Me_nPh_{3-n}P)_3M(\eta^1\text{-}SO_2)$ species ($n = 1-3$). The minima found during these tests were used as starting points for the DFT optimizations.

DFT Optimizations. Since using a triple-ζ + polarization (TZP) basis set on all atoms of a $(Me_nPh_{3-n}P)_3M(\eta^1\text{-}SO_2)$ complex ($n \neq 3$) would have been resource-prohibitive, we examined a series of smaller basis sets to find one that would perform adequately for less cost. We did so by determining the interaction energies ΔE_{int}[22] of the three $(Me_3P)_3M(\eta^1\text{-}SO_2)$ complexes using the TZP basis set on all atoms. We then reoptimized the complexes and redetermined the ΔE_{int} values using several less demanding basis sets. The data for $(Me_3P)_3Pt(\eta^1\text{-}SO_2)$ appear in Table 2. One sees that the TZP/DZ/DZ basis set gives values within 0.5 kcal mol^{-1} of those from the TZP basis set with considerably fewer basis functions required. The still less demanding TZP/SZ/SZ, DZ/DZ/DZ basis sets, and the QMMM approach, perform far less well. From these data and those for the other tris(trimethylphosphine) compounds, the TZP/DZ/DZ basis set was judged to best combine accuracy (compared to the TZP basis set) with efficient resource usage.

Once fully DFT-optimized structures (Table 3) were obtained from the starting points obtained from the QMMM studies above,

(10) Amsterdam Density Functional program, Division of Theoretical Chemistry, Vrije Universiteit, De Boelelaan 1083, 1081 HV Amsterdam, The Netherlands; http://www.scm.com.
(11) (a) Baerends, E. J.; Ellis, D. E.; Ros, P. *Chem. Phys.* **1973**, *2*, 41−51. (b) Baerends, E. J.; Ros, P. *Chem. Phys.* **1973**, *2*, 52−59.
(12) Ravenek, W. In *Algorithms and Applications on Vector and Parallel Computers*; te Riele, H. J. J., Dekker, T. J., van de Horst, H. A., Eds.; Elsevier: Amsterdam, The Netherlands, 1987.
(13) (a) te Velde, G.; Baerends, E. J. *J. Comput. Chem.* **1992**, *99*, 84−98. (b) Boerrigter, P. M.; te Velde, G.; Baerends, E. J. *Int. J. Quantum Chem.* **1988**, *33*, 87−113.
(14) Versluis, L.; Ziegler, T. *J. Chem. Phys.* **1988**, *88*, 322−328.
(15) Vosko, S. H.; Wilk, L.; Nusair, M. *Can. J. Phys.* **1980**, *58*, 1200−1211.
(16) Perdew, J. P.; Chevary, J. A.; Vosko, S. H.; Jackson, K. A.; Pederson, M. R.; Singh, D. J.; Fiolhais, C. *Phys. Rev. B* **1992**, *46*, 6671−6687.
(17) Snijders, J. G.; Baerends, E. J.; Ros, P. *Mol. Phys.* **1979**, *38*, 1909−1929.
(18) Van Lenthe, E.; van Leeuwen, R.; Baerends, E. J.; Snijders, J. G. *Int. J. Quantum Chem.* **1996**, *57*, 281.
(19) Clark, M.; Cramer, R. D., III; Van Opdenbosch, N. *J. Comput. Chem.* **1989**, *10*, 982−1012.
(20) Rappé, A. K.; Casewit, C. J.; Colwell, K. S.; Goddard, W. A., III; Skiff, W. M. *J. Am. Chem. Soc.* **1992**, *114*, 10024−10035.

(21) For example, the QMMM-predicted average P−C distance in $(Ph_3P)_3Pt(\eta^1\text{-}SO_2)$ is 1.828 Å; the experimental average is 1.835(9) Å. The QMMM-predicted average P−C_{methyl} and P−C_{phenyl} distances in $(Me_2PhP)_3Ni(\eta^1\text{-}SO_2)$ are 1.825 and 1.840 Å, respectively; the corresponding experimental values are 1.836(7) and 1.818(5) Å

(22) ΔE_{int} is the energy associated with breaking the bond between the fragments but not letting them relax to their equilibrium geometries. See the subsection describing bond energy decomposition. Computationally, ΔE_{int} was determined by optimizing a particular $(Me_3P)_3M(\eta^1\text{-}SO_2)$ molecule, determining its single point energy, and then determining the single point energy of the trigonal pyramidal $(Me_3P)_3M$ fragment from the optimization rather than optimizing the fragment to its trigonal planar isomer. Thus, the PW91/TZP/TZP/TZP value given for $(Me_3P)_3Pt(\eta^1\text{-}SO_2)$ in Table 2 is the ΔE_{int} value and differs from the "true" BDE in Table 4.

Table 2. Predicted (PW91) ΔE_{Int} Values (kcal mol^{-1}) for $(Me_3P)_3Pt(\eta^1\text{-}SO_2)$ Using Various Basis Sets

basis set on Pt, S, P, O	basis set on C	basis set on H	basis functions	BDE
TZP	TZP	TZP	554	34.9
TZP	QMMM	QMMM		21.3
TZP	SZ	SZ	293	46.0
TZP	DZ	SZ	255	32.4
TZP	DZP	SZ	383	31.9
TZP	TZP	SZ	419	34.0
TZP	DZ	DZ	356	34.6
TZP	DZP	DZ	410	34.8
DZ	DZ	DZ	285	56.5

Table 3. Selected Predicted (PW91) and Experimental Structural Data for $(H_3P)_3M$, $(H_3P)_3M(\eta^1\text{-}SO_2)$, $(Ph_nMe_{3-n}P)_3M$, and $(Ph_nMe_{3-n}P)_3M(\eta^1\text{-}SO_2)$ Complexes[a]

(a) $(R_3P)_3M$ M−P Distances

R_3P	Ni	Pd	Pt
H_3P	2.133	2.317	2.282
Me_3P	2.140	2.325	2.293
Me_2PhP	2.132	2.311	2.282
Ph_2MeP	2.131	2.305	2.281
Ph_3P	2.144	2.323	2.288
expt	2.147(6)[b]	2.316(5)[c]	2.266(2)[d]

(b) $(R_3P)_3M(\eta^1\text{-}SO_2)$

	M−P	M−S	τ_{MSO_2}
$(H_3P)_3Ni(\eta^1\text{-}SO_2)$	2.181	2.075	178.4
$(H_3P)_3Pd(\eta^1\text{-}SO_2)$	2.377	2.438	120.9
$(H_3P)_3Pt(\eta^1\text{-}SO_2)$	2.323	2.504	115.9
$(Me_3P)_3Ni(\eta^1\text{-}SO_2)$	2.194	2.058	164.3
$(Me_3P)_3Pd(\eta^1\text{-}SO_2)$	2.381	2.368	137.2
$(Me_3P)_3Pt(\eta^1\text{-}SO_2)$	2.341	2.387	136.9
$(Me_2PhP)_3Ni(\eta^1\text{-}SO_2)$	2.195	2.055	172.9
expt[e]	2.202 (3)	2.001 (3)	142.6
$(Me_2PhP)_3Pd(\eta^1\text{-}SO_2)$	2.366	2.339	138.4
$(Me_2PhP)_3Pt(\eta^1\text{-}SO_2)$	2.328	2.360	138.5
$(Ph_2MeP)_3Ni(\eta^1\text{-}SO_2)$	2.200	2.061	170.7
$(Ph_2MeP)_3Pd(\eta^1\text{-}SO_2)$	2.379	2.352	136.6
$(Ph_2MeP)_3Pt(\eta^1\text{-}SO_2)$	2.341	2.343	146.7
$(Ph_3P)_3Ni(\eta^1\text{-}SO_2)$	2.237	2.084	161.0
expt[f]	2.260 (4)	2.038 (4)	166.9
$(Ph_3P)_3Pd(\eta^1\text{-}SO_2)$	2.399	2.436	125.9
$(Ph_3P)_3Pt(\eta^1\text{-}SO_2)$	2.358	2.486	120.1
expt[g]	2.348 (2)	2.368 (3)	123.0

[a] Bond distances in Å, angles in deg. [b] Dick, D. G.; Stephan, D. W.; Campana, C. F. *Can. J. Chem.* **1990**, *68*, 628−632. [c] Sergienko, V. S.; Porai-Koshits, M. A. *Zh. Strukt. Khim.* **1987**, *28* (4), 103−106. [d] Chaloner, P. A.; Hitchcock, P. B.; Broadwood-Strong, G. T. L. *Acta Crystallogr.* **1989**, *C45*, 1309−1311. [e] Sieler, J.; Peters, K.; Wenschuh, E.; Hoffmann, T. *Z. Anorg. Allg. Chem.* **1987**, *549*, 171−176. [f] Moody, D. C.; Ryan, R. R. *Inorg. Chem.* **1979**, *18*, 223−227. [g] Eller, P. G.; Ryan, R. R.; Moody, D. C. *Inorg. Chem.* **1976**, *15*, 2442−2445.

Table 4. Predicted (PW91) M−S Bond Dissociation Energies (kcal mol^{-1}) for $(H_3P)_3M(\eta^1\text{-}SO_2)$ and $(Ph_nMe_{3-n}P)_3M(\eta^1\text{-}SO_2)$ Complexes

R_3P	Ni	Pd	Pt
H_3P	28.0	14.6	15.1
Me_3P	37.0	24.2	24.4
Me_2PhP	35.5	25.8	25.0
Ph_2MeP	37.0	21.5	22.9
Ph_3P	25.2	15.8	14.5

M−S bond dissociation energies (BDEs) were calculated by subtracting the sum of the energies of the L_3M fragment and of SO_2 from the energy of the $L_3M(\eta^1\text{-}SO_2)$ molecule. These appear in Table 4. The data were not corrected for basis set superposition error (BSSE), because the correction at this basis set level is probably $\leq$2.0 kcal mol^{-1},[23] and because it is probably systematic across the series of molecules investigated, and thus will not affect comparisons. They are corrected for scalar relativistic effects only, as the cost of single-point spin−orbit relativistic calculations for the polyphenyl-substituted phosphine compounds proved prohibitive.

The full DFT optimization approach was used for scans of the potential energy surface involving rotation of the SO_2 moiety with respect to the M−P_3 "Y" (orientation scans) and pyramidalization of the sulfur atom (conformation scans), for the series $(H_3P)_3M(\eta^1\text{-}SO_2)$, $(Me_3P)_3M(\eta^1\text{-}SO_2)$, $(Me_2PhP)_3M(\eta^1\text{-}SO_2)$. The first two sets employed the TZP basis set on all atoms; the last set used the TZP/DZ/DZ basis set.

As the calculated structures typically exhibit expected bond distances and angles, particularly for the spectator ligands, only notable parameters are given in the text and tables below. Cartesian coordinates for all species studied are available as Supporting Information.

Bond Energy Decomposition. The approach has been described in several places,[24] so we describe it only briefly. The BDE is decomposed to terms as follows:

$$\Delta E_{BDE} = \Delta E_{prep} + \Delta E_{int} = \Delta E_{prep} + \Delta E_{elstat} + \Delta E_{Pauli} + \Delta E_{orbital}$$

where ΔE_{prep} is the energy associated with deforming the fragments of interest to their geometries in the molecule/ion, ΔE_{elstat} is the electrostatic interaction energy between the fragments, ΔE_{Pauli} is the repulsive interaction energy between the fragments resulting from interactions between occupied orbitals, and $\Delta E_{orbital}$ is the energy associated with relaxation of the Kohn−Sham orbitals as self-consistency is reached. ΔE_{elstat} and $\Delta E_{orbital}$ broadly describe electrostatic and covalent attractive aspects of bonding, respectively, while ΔE_{Pauli} describes repulsive aspects. For the systems here, ΔE_{prep} is generally on the order of 10 kcal mol^{-1}, a sizable fraction of the overall BDE. This corresponds to the pyramidal $(R_3P)_3M$ fragment relaxing to the less congested trigonal planar conformer. The ΔE_{int} values, which are BDEs associated with simply breaking the M−S bond, and not allowing the fragments to relax, are therefore about 10 kcal mol^{-1} larger than those in Table 4.

Results and Discussion

Structures and Conformational/Orientation Energies. Selected bond length and angle data for the tris(phosphine) metal fragments and the corresponding SO_2 complexes appear in Table 3. The model predicts bond lengths and angles in good agreement with experiment, where such data exist. M−P distances are modeled particularly well. One notes that these distances vary little over the range of phosphines for a particular metal, despite their differing basicities and steric requirements. The only detectable exception is that the M−P distances for the $(Ph_3P)_3M(\eta^1\text{-}SO_2)$ complexes are 0.02−0.03 Å longer than those for systems with less bulky phosphines.

Experimental and computational results disagree notably in two areas: the pyramidality of the S atom in $(Me_2PhP)_3Ni$-

(23) ADF examples manual for loss of CO from $Cr(CO)_6$, available from http://www.scm.com.

(24) (a) Diefenbach, A.; Bickelhaupt, F. M.; Frenking, G. *J. Am. Chem. Soc.* **2000**, *122*, 6449−6458. (b) Szilagyi, R.; Frenking, G. *Organometallics* **1997**, *16*, 4807−4815. (c) Ziegler, T. *Can. J. Chem.* **1995**, *73*, 743−761. (d) Ziegler, T. *Chem. Rev.* **1991**, *91*, 651−667. (e) Ziegler, T. In *Metal−Ligand Interactions: from Atoms to Clusters to Surfaces*; Salahub, D. R., Russo, N., Eds.; Kluwer: The Netherlands, 1992, 367−396.

(η^1-SO_2) and the M−S bond lengths. The former is of interest, because Wenschuh et al. have considered this and the analogous $(Et_2PhP)_3Ni(\eta^1\text{-}SO_2)$ as unique among $(R_3P)_3Ni(\eta^1\text{-}SO_2)$ compounds in adopting extremely pyramidal SO_2 conformations.[6] The characterization derives from ready dissociation of SO_2 from the metal fragment, and a single-crystal X-ray diffraction study of $(Me_2PhP)_3Ni(\eta^1\text{-}SO_2)$, which refined to a structure containing a pyramidal SO_2 that unfortunately was also disordered and therefore geometrically suspect.

Our observation that all the $(R_3P)_3Ni(\eta^1\text{-}SO_2)$ complexes are predicted to display nearly planar SO_2 conformations suggests that the disorder in the X-ray study gave a spurious result, and that the geometry around the sulfur is actually (nearly) planar. However, scans of the potential energy surface for pyramidalization of the sulfur atom provide an alternative possibility. They reveal that surprisingly little energy is required to pyramidalize the sulfur in any of the nickel compounds, or to flatten the sulfur in the palladium and platinum compounds. For example, the energy difference between $(H_3P)_3Ni(\eta^1$-perfectly planar $SO_2)$ (defined as having an angle τ_{NiSO_2} of 180.0° between the Ni−S vector and the SO_2 plane) and $(H_3P)_3Ni(\eta^1$-highly pyramidal $SO_2)$ ($\tau_{NiSO_2} = 120°$) is only 5.8 kcal mol^{-1}. The values for the more electron-rich (and more experimentally plausible) $(Me_n\text{-}Ph_{3-n}P)_3Ni(\eta^1\text{-}SO_2)$ complexes are 4.3 kcal mol^{-1} ($n = 3$), 3.5 kcal mol^{-1} ($n = 2$), 5.9 kcal mol^{-1} ($n = 1$), and 2.2 kcal mol^{-1} ($n = 0$). The last two values are somewhat coarse estimates since the QMMM approach was used for these scans, but they are in line with the others. Even these small energies are misleading. In the context of the experimental results, we note that $(Ph_3P)_3Ni(\eta^1\text{-}SO_2)$ with $\tau_{NiSO_2} = 166°$ (the experimental value) is only 0.66 kcal mol^{-1} more stable than the conformer with $\tau_{NiSO_2} = 180°$ and 1.9 kcal mol^{-1} more stable than that with $\tau_{NiSO_2} = 140°$. Similarly, $(Me_2\text{-}PhP)_3Ni(\eta^1\text{-}SO_2)$ with $\tau_{NiSO_2} = 140°$ (nearly the experimental value) is 0.20 kcal mol^{-1} more stable than the conformer with $\tau_{NiSO_2} = 180°$ and only 1.3 kcal mol^{-1} less stable than the computationally optimized molecule with $\tau_{NiSO_2} = 170°$. In general, changes in τ_{MSO_2} of ±20° from the predicted equilibrium value require less than 1.0 kcal mol^{-1} in energy. This suggests that the pyramidal sulfur atom observed in the X-ray study of $(Me_2PhP)_3Ni(\eta^1\text{-}SO_2)$ could be correct despite the disorder, but that this geometry is adopted as a result of solid state effects rather than being a molecular equilibrium state.

To support the argument from the other direction, we note that the energy required to planarize the sulfur (from $\tau_{PtSO_2} = 120°$ to 180°) in $(R_3P)_3Pt(\eta^1\text{-}SO_2)$ complexes ranges from 1.5 kcal mol^{-1} (PH_3) to 4.7 kcal mol^{-1} (PMe_3) to 2.7 kcal mol^{-1} (PMe_2Ph) to 3.8 kcal mol^{-1} (PPh_2Me) to 3.5 kcal mol^{-1} (PPh_3). Thus, even though all Pd and Pt complexes adopt geometries containing a pyramidal sulfur, the observed τ_{MSO_2} will certainly depend on the environment if observed in a condensed phase. It is therefore gratifying that the model predicts τ_{PtSO_2} for $(Ph_3P)_3Pt(\eta^1\text{-}SO_2)$ in excellent agreement with experiment.

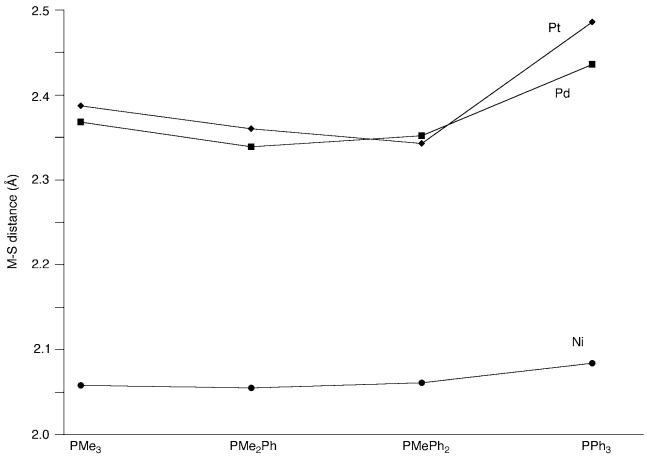

Figure 1. Variation of the M−S bond distance (Å) with phosphine ligand for $(Me_nPh_{3-n}P)_3M(\eta^1\text{-}SO_2)$ complexes (M = Ni, Pd, Pt; $n = 0-3$).

The model overestimates the M−S bond distance slightly for $(Me_2PhP)_3Ni(\eta^1\text{-}SO_2)$ and $(Ph_3P)_3Ni(\eta^1\text{-}SO_2)$ (ca. 0.05 Å) and substantially for $(Ph_3P)_3Pt(\eta^1\text{-}SO_2)$ (0.12 Å). Some of this discrepancy may lie in a systematic error associated with the PW91 model. Workers have previously observed that gradient-corrected DFT models such as PW91 and RPBE tend to slightly overestimate metal−ligand bond lengths.[25] However, some of the difference reflects a very flat potential energy surface corresponding to stretching/compressing the M−S bond. We probed this using a QMMM scan of the Pt−S distance in $(Ph_3P)_3Pt(\eta^1\text{-}SO_2)$. Over the range 2.49−2.37 Å (corresponding essentially to the discrepancy between computational and experimental distances), the molecular energy changed by only 0.75 kcal mol^{-1}. Because this estimate is coarse owing to the use of QMMM, we confirmed it briefly by optimizing $(Ph_3P)_3Pt(\eta^1\text{-}SO_2)$ using the full DFT PW91/TZP/DZ/DZ approach with the Pt−S distance fixed at 2.37 Å. The energy difference between the constrained and unconstrained molecules was essentially nil. These data indicate that stretching or compressing the Pt−S bond requires little energy, and thus, the difference between the gas phase computational result and solid state experimental result probably arises from condensed phase effects, with possibly a small error from the model.

We note that the model predicts the apparent increase in M−S bond length with phenyl substitution on the phosphine ligand for the $(Me_nPh_{3-n}P)_3M(\eta^1\text{-}SO_2)$ complexes. One sees in Table 3 that the experimental bond distance in $(Ph_3P)_3\text{-}Ni(\eta^1\text{-}SO_2)$ is 0.037 Å longer than that in $(Me_2PhP)_3Ni(\eta^1\text{-}SO_2)$, while computationally the difference is 0.029 Å. The data appear in graphical form in Figure 1. One sees that the M−S bond lengths vary slightly from $PR_3 = PMe_3$ to $PMePh_2$, and then increase somewhat for Ni and dramatically for Pd and Pt when $PR_3 = PPh_3$. This mimics the behavior of the BDEs for these species, which we discuss below.

We undertook scans of the potential energy surface corresponding to rotation of the SO_2 moiety with respect to the M−P_3 "Y" because optimizations of Pd and Pt complexes failed to show marked preferences for staggered or eclipsed

(25) Ziegler, T. *J. Chem. Soc., Dalton Trans.* **2002**, 642−652.

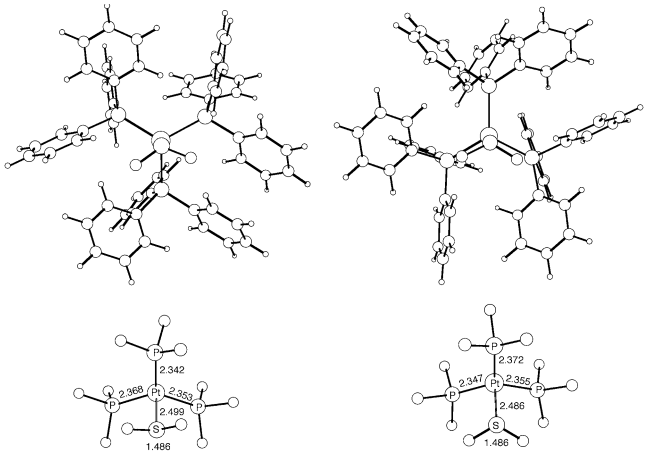

Figure 2. View of the predicted (PW91/TZP/DZ/DZ) structures of the staggered (left) and eclipsed (right) rotamers of $(Ph_3P)_3Pt(\eta^1\text{-}SO_2)$ down the Pt−S axis. The smaller graphics show the molecular core and include some bond distances in Å.

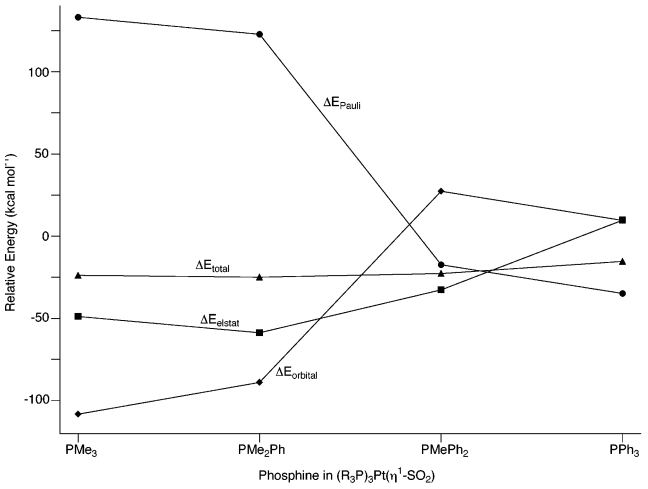

Figure 3. Relative energies (PW91/TZP/DZ/DZ, kcal mol^{-1}) of the terms in the bond energy decomposition for the reactions $(Me_nPh_{3-n}P)_3Pt(\eta^1\text{-}SO_2) \rightarrow (Me_nPh_{3-n}P)_3Pt + SO_2$ ($n = 0-3$).

orientations. An example, $[(Ph_3P)_3Pt(\eta^1\text{-}SO_2)]$, appears in Figure 2. The two rotamers differ by only 0.21 kcal mol^{-1} at the PW91/TZP/DZ/DZ level. Scans over the torsion angle connecting the two orientations for all the SO_2 complexes showed this to be general, with the energy span over the scan never exceeding 1 kcal mol^{-1}. Thus, no barrier to rotation around the M−S bond exists; whatever conformation was observed in the single crystal diffraction studies generally depended on condensed phase forces, and possibly on random chance.

Bond Dissociation Energies (BDEs). The predicted M−S bond dissociation energies (BDEs) appear in Table 4. The BDEs for the nickel complexes are similar to those estimated for "middle-of-the-transition series" d^6 $(CO)_5M(\eta^1\text{-}SO_2)^{nq}$ complexes (M = V−Ta, $nq = 1-$; M = Cr−W, $nq = 0$; M = Mn−Re, $nq = 1+$).[9a] These, like the Ni complexes, exhibit a planar SO_2 ligand. The Pd and Pt complexes, which contain pyramidal SO_2, show much lower BDEs, typically 50−70% of those for Ni. This confirms the view that pyramidality translates to greater lability and reactivity at sulfur, and puts it on a more quantitative basis.

Unfortunately, no experimental BDEs exist to compare these with. However, the smaller BDE for Pt compared to Ni is consistent with the surface absorption data of Rodriguez et al.[26] The BDEs for the Pt complexes are also similar to those calculated for $\eta^1\text{-}SO_2$ binding to the Pt (111) surface (11−23 kcal mol^{-1}) by Trout et al.[27]

An intriguing aspect of the BDEs is their lack of variation from the tris(PMe_3) complexes to the tris(PPh_2Me) complexes, and then their substantial drop for the tris(PPh_3) complexes. One might have expected a more linear decline as the basicity of the ligand decreases as the number of phenyl groups increases.[28] Hirschfeld charge analysis suggests that the metals experience a fairly smooth change in local electron density. For example, for the $(Me_nPh_{3-n}P)_3Pt(\eta^1\text{-}SO_2)$ series, the model suggests that the charge on Pt varies from −0.016 (PMe_3) to 0.010 (PMe_2Ph) to 0.020 (PPh_2Me) to 0.046 (PPh_3), while the charges on the P atoms remain nearly constant at ca. 0.2 e$^-$. We attempted to probe the anomaly quantitatively, using the energy decomposition data available in ADF output. The data appear graphically for the $(Me_nPh_{3-n}P)_3Pt(\eta^1\text{-}SO_2)$ series in Figure 3. (Note that, conventionally, attractive energies are given negative values, so the BDEs, shown as ΔE_{total}, are negative.) One sees that the values do not vary smoothly, and that the individual terms ΔE_{Pauli}, ΔE_{elstat}, and $\Delta E_{orbital}$ do not track the ΔE_{total} trend well. $\Delta E_{orbital}$, which broadly represents covalent bonding interactions, does decrease with increasing number of phenyl groups, consistent with the view that phosphine basicity changes similarly. ΔE_{Pauli} follows this as well, with repulsion energy decreasing (although not smoothly) with the number of phenyl substituents (decreasing basicity). Unfortunately, we have been unable to create a self-consistent picture of the relationship between phosphine basicity and M−S BDE using these data. We suspect this reflects the dependence of phosphine basicity on both steric and electronic factors.[28] Furthermore, we caution the reader that the values of the ΔE terms represent small differences between large numbers.[29] As a result, inadequate cancellation of errors when determining the large numbers can result in the small differences being meaningless.

It may be that the BDE does not greatly reflect the basicity of the phosphine, but correlates more with the steric demands of the phosphine ligands. Qualitatively, one can argue the $M-SO_2$ bond weakens only slightly as PR_3 changes from PMe_3 to $PMePh_2$ because the methyl groups and the SO_2 oxygens act like meshing gears as the phosphines rotate around the M−P axes. (Recall that rotation of the SO_2 moiety

(26) Rodriguez, J. A.; Hrbek, J. *Acc. Chem. Res.* **1999**, *32*, 719−728.
(27) Lin, X.; Hass, K. C.; Schneider, W. F.; Trout, B. L. *J. Phys. Chem. B* **2002**, *106*, 12575−12583.

(28) One should note, however, that the gas-phase proton affinities and gas-phase basicities of the phosphines do not vary linearly. The data, taken from the NIST Web Book (http://webbook.nist.gov), are as follows. Gas-phase proton affinities: PMe_3, 958.8 kJ mol^{-1}; PMe_2Ph, 969.2 kJ mol^{-1}; $PMePh_2$, 972.1 kJ mol^{-1}; PPh_3, 972.8 kJ mol^{-1}. Gas-phase basicities: PMe_3, 926.3 kJ mol^{-1}; PMe_2Ph, 936.8 kJ mol^{-1}; $PMePh_2$, 939.7 kJ mol^{-1}; PPh_3, 940.4 kJ mol^{-1}.
(29) For example, the value of ΔE_{Pauli} for $(Ph_2MeP)_3Pt(\eta^1\text{-}SO_2)$ derives from the subtraction (47586.87 − 46076.65 − 1527.69) kcal mol^{-1}.

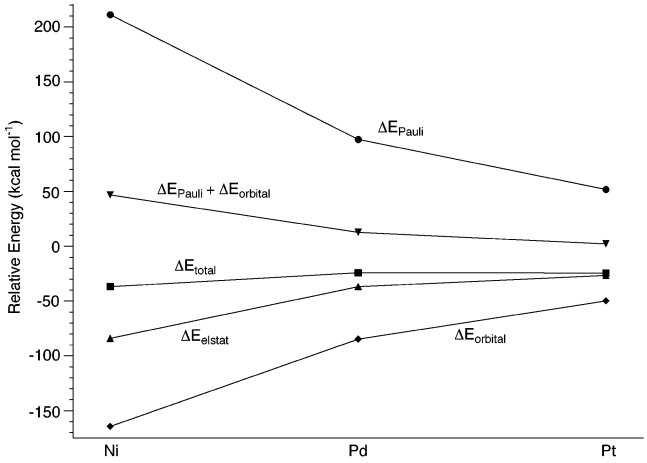

Figure 4. Relative energies (PW91/TZP, kcal mol^{-1}) of the terms in the bond energy decomposition for the reactions $(Me_3P)_3M(\eta^1\text{-}SO_2) \rightarrow (Me_3P)_3M + SO_2$ (M = Ni, Pd, Pt).

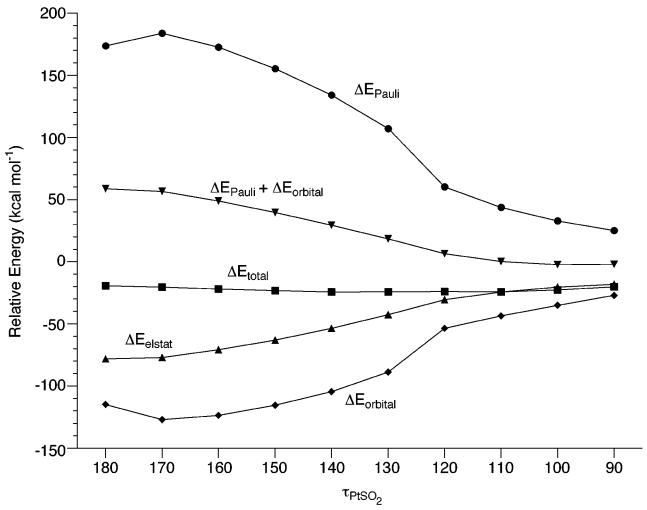

Figure 5. Relative energies (PW91/TZP, kcal mol^{-1}) of the terms in the bond energy decomposition for the process of pyramidalizing the SO_2 ligand in $(Me_3P)_3Pt(\eta^1\text{-}SO_2)$.

requires little energy.) However, in the tris(PPh_3) complexes this meshing effect is lost, so the steric demands of the phosphine ligands "push" the SO_2 ligand out, dramatically weakening the M−S bond. This correlates with the observation that the M−S bond distances tend to change little as the ligand changes from PMe_3 to $PMePh_2$, then lengthen dramatically for $PR_3 = PPh_3$.

A plot of the components of the BDE versus the metal for the $(Me_3P)_3M(\eta^1\text{-}SO_2)$ series (Figure 4) reveals some interesting trends. One sees that the component energies for the Ni complex differ substantially from those for the Pd and Pt complexes, which are similar. This correlates with the different SO_2 geometries adopted by the complexes. For the former, the three components contribute differently to the overall ΔE_{total}, so that no one term determines the sum. In contrast, for the latter pair ΔE_{Pauli} and $\Delta E_{orbital}$ nearly cancel, so that ΔE_{total} is determined by the electrostatic term ΔE_{elstat}. This observation is supported by the bond decomposition data for the process of bending the SO_2 ligand in $(Me_3P)_3Pt(\eta^1\text{-}SO_2)$ (Figure 5). One sees that as τ approaches the predicted equilibrium value of ca. 120°, the sum $\Delta E_{Pauli} + \Delta E_{orbital}$ goes to zero, so that ΔE_{elstat} and ΔE_{total} become identical. Thus the M−pyramidal SO_2 BDE in a d^{10} system is largely determined by the value of ΔE_{elstat}. Since this term is generally small relative to the other two, the observation implies that SO_2 bound in a pyramidal fashion will generally exhibit a smaller BDE than SO_2 bound in a planar fashion. This is in accord with the experimental findings mentioned above.

That the Pd/Pt complexes contain pyramidal SO_2 ligands accounts for ca. 3−5 kcal mol^{-1} (the energy associated with flattening the SO_2 in a Pd or Pt complex) of the bond energy difference between Ni and Pd/Pt complexes. There remains a 5−14 kcal mol^{-1} difference in BDE to account for. Inspection of Figure 4 shows that the orbital-based components ΔE_{Pauli} and $\Delta E_{orbital}$ exhibit much larger values for Ni than for the others, implying that orbital interactions are greater for this system over and above those associated with the issue of planar versus pyramidal SO_2. This must stem from better energy matching of the bonding S and Ni orbitals as compared with S/Pd and S/Pt orbitals, owing to the proximity of the former in the periodic table. Such a view is not trivial to test within the confines of the model. However, one approach involves examining the atom−atom overlap population for the metal−sulfur bonds. We did this for the three $(Me_3P)_3M(\eta^1\text{-}SO_2)$ complexes, optimized with τ_{MSO_2} constrained to 180°. The overlap populations are 0.352 for Ni−S, 0.310 for Pd−S, and 0.248 for Pt−S. One must view these values with caution, since they depend somewhat on the bond distance, but the trend is consistent with that expected for poorer orbital energy matching as one moves down the family.

Conclusions

The calculations described here quantify the difference between planar and pyramidal SO_2 bound to a d^{10} $(R_3P)_3M$ fragment to 3−5 kcal mol^{-1}. Combined with the improved orbital overlap associated with Ni−S interactions versus Pd−S or Pt−S interactions, this translates to a 10−17 kcal mol^{-1} stronger bond for the former. However, none of the M−S bonds are exceptionally strong, so much broader reaction chemistry than has so far been discovered might be available to these systems. That the Ni complexes employ sizable electrostatic and covalent interactions in bonding means that they might activate SO_2 toward electrophilic or nucleophilic attack (although this evidently does not hold as regards attack by O_2). Given the low cost of nickel, exploring its use as a possible broad-range catalyst for SO_2 remediation seems worthy.

Acknowledgment. The NIU Computational Chemistry Laboratory (NIU CCL) is supported in part by the taxpayers of the State of Illinois and by U.S. Department of Education Grant P116Z020095.

Supporting Information Available: Cartesian coordinates and absolute energies of all molecules examined at the applicable model levels. This material is available free of charge via the Internet at http://pubs.acs.org.

IC030229Q